The groundwater environmental effects and health risk assessment in saline-fresh water mixing zone of coastal plain

Sen Liu (sen_liu@sdu.edu.cn)
Shandong University
Xiao Yang
Shandong University
Yanan Liu
Shandong University
Chao Jia
Shandong University
Maosheng Gao
Qingdao Institute of Marine Geology
Xianzhang Dang
Qingdao Institute of Marine Geology

Research Article

Keywords: Groundwater environment, saline water intrusion, high-F groundwater, health risk, coastal plain

Posted Date: March 17th, 2022

DOI: https://doi.org/10.21203/rs.3.rs-1351790/v1

Title Page

The groundwater environmental effects and health risk assessment in saline-fresh water mixing zone of coastal plain

Sen Liu [a, b*1], Xiao Yang [a, 1], Yanan Liu [a], Chao Jia [a], Maosheng Gao [c], Xianzhang Dang [c, d]

a, Institute of Marine Science and Technology, Shandong University, Qingdao, 266237, China

b, State Key Laboratory of Estuarine and Coastal Research, East China Normal University, Shanghai, 200062, China

c, Qingdao Institute of Marine Geology, CGS, Qingdao 266071, China.

d, School of Environmental Studies, China University of Geosciences, 388 Lumo Rd, Wuhan, 430074, China

[1] These authors contributed equally to this work.

*Corresponding author: Sen Liu (sen_liu@sdu.edu.cn, luicent@sina.com)

Corresponding address: Institute of Marine Science and Technology, Shandong University, Binhai Road NO. 72. Qingdao, Shandong Province, CHINA

Phone Numbers: +86 15898868448

Postal Address: Shandong University, Binhai Road NO. 72. Qingdao, Shandong Province, CHINA

Abstract: The groundwater environment is important to human living in coastal plain. In this study, southern Laizhou Bay (SLB) is chosen as the study area and 47 groundwater samples are collected to analyze groundwater environmental effects and health risk assessment in saline-fresh water mixing zone (SFMZ) of coastal plain. Influenced by saline water intrusion (SWI), K^+, Na^+, Ca^{2+}, Mg^{2+}, Cl^-, SO_4^{2-} and HCO_3^- concentration values are exceeded WHO standard value seriously. High-F groundwater is the product in process of SWI, caused by cation exchange, weakly alkaline environment, evaporation and fluorite dissolution. Na^+ concentration and a decrease in the Ca^{2+} concentration can promote further dissolution of fluorite and other F-containing minerals. Based on the health risk assessment method, the average HQ sequence in typical groundwater pollutants is Cl^- > F^- > NO_3-N > Se > Mn > NO_2-N > Cu > Pb > Zn > Fe, and the CR sequence caused by carcinogenic heavy metals is Cd > As > Cr. The greatest non-carcinogenic risk to adults and children in the study area is caused by Cl^-. Cd is the most important indicator of carcinogenic risk, and its contribution to CR accounts for 74.531%. The regions with high health impacts of carcinogenic pollutants in groundwater are mainly concentrated in the central part of the study area, with the exceeding range of 35.373% for adults and 44.768% for children. Non-carcinogenic pollutants are enriched in SFMZ, which have greater impacts on human body and lead to higher health risks compared with carcinogenic pollutants.

Keywords: Groundwater environment; saline water intrusion; high-F groundwater; health risk; coastal plain.

Highlights

1. High-F groundwater is the product in process of SWI.

2. Human activities and natural conditions can affect the groundwater environment in coastal plain.

3. Ensure the main pollutants to HQ and CR.

1. Introduction

Water resources, especially for groundwater resource, are an indispensable natural resource for human survival and development and an important part of ecological and environmental systems in coastal plain (Post, 2005; Al-Ansari, 2013; Adimalla and Qian, 2021; Wang et al., 2021). The cleanliness and safety of groundwater are directly related to human health (Sanford and Pope, 2010; Famiglietti, 2014). Due to agriculture, industry, economic development and population growth, the consumption of groundwater resource has accelerated and groundwater contamination, which is a gradual and hazardous process with negative effects, has been a common environmental problem worldwide (Wen et al., 2019; Lu et al., 2020; Li et al., 2021; Wang et al., 2021; Solgi and Jalili., 2021). Heavy metal pollution, fluorine, nitrate, organic pollutants and groundwater salinization are the main groundwater pollutants and have been a hidden threat to human health for a long time.

Numerous studies have been carried out to analyze groundwater genetic mechanisms, groundwater quality evaluations and human health risk assessments (Li et al., 2017, 2018; Luo et al., 2021). High-F groundwater is the most widespread cause of fluorosis worldwide, such as the United States, India, Pakistan, South Africa, South Korea and China (Chae et al., 2007; Kim et al., 2012; Lü et al., 2016; Thapa et al., 2018; Jia et al., 2019; Yadav et al., 2019; Mcmahon et al., 2020). Arsenic has been widely recognized as among the most toxic chemicals, and over 200 million people worldwide still drink arsenic-contaminated water (Naujokas et al., 2013). High NO_3-N

concentrations can lead to methemoglobinemia or blue baby syndrome (Rezaei et al., 2019). Heavy metals, such as Cd, Cr, and As, can damage the human nervous, digestive, and endocrine systems and may induce cancer (Sharma et al., 2019; Manoj et al., 2021; Mukherjee et al., 2021). Some heavy metals inhibit the activity of enzymes, causing cytoplasmic poisoning, thus affecting nerve tissue and even damaging the key organs of human detoxification (Sharma et al., 2014; Wang et al., 2021). The safety of water resource quality has become very important to human health.

In this study, we are focused on a typical groundwater environmental issue, saline water intrusion, in coastal plain. Saline water intrusion (SWI), caused by overexploitation of groundwater, is the common groundwater environmental issue in coastal plain (Liu et al., 2017). Different from seawater intrusion which is the mixing process between seawater and groundwater, SWI is the mixing process between underground saline water and fresh water in groundwater environment and away from coastline. It can change the properties of groundwater environment, such as ion exchange and groundwater salinization, which can lead to increase of TDS and Cl^- concentrations and enrichment of high-fluorine groundwater (Gao et al., 2017; Liu et al., 2017; Chen et al., 2019, 2020). A saline-fresh water mixing zone (SFMZ) has formed under the condition of SWI.

Southern Laizhou Bay (SLB), which was chosen as the study area, is a typical coastal plain and an important salt production base in China. Groundwater with different water quality type is distributing widely in this area, such fresh water, brackish water, saline water and brine (Liu et al., 2016, 2017; Yang et al., 2021). SWI is the main

groundwater environmental problem and SFMZ has formed. Forty-seven groundwater samples, which were distributed in the SFMZ, were collected to obtain heavy metal and hydrochemical data. The objectives of this study were to (1) further investigate and analyze the spatial distribution characteristics of main pollutions and hydrochemical data in the groundwater environment of the SFMZ; (2) evaluate the human health risk of groundwater and analyze the main influencing factors; and (3) explore the groundwater environmental effects in SFMZ. The research results can provide a scientific reference for groundwater resource management, heavy metal pollution control, and ensuring drinking water safety in coastal plains.

2. Materials and methods

2.1 Background of study area

2.1.1 Location and climatic conditions of study area

The SLB is located in the southern Bohai Sea and northern Weibei Plain, Shandong Province, China (Fig. 1). The landform types consist of coastal plains, shoals and intertidal zones from south (land) to north (sea), with ground surface elevations ranging from 500 m to 1 ~ 2 m. The broad alluvial plain has been shaped by several rivers, such as the Bailang River, Wei River and Mi River. The average annual precipitation is approximately 660 mm, and 60% – 70% of the rainfall occurs between June and August. The mean annual evaporation is 1648 mm, with 50% of the total evaporation capacity occurring from April to June (Liu et al., 2016).

2.1.2 Hydrochemical types of groundwater

In this study area, groundwater are divided into four classes: fresh water (TDS <

1 g/L), brackish water (1 g/L ≤ TDS < 3 g/L), saline water (3 g/L ≤ TDS < 50 g/L) and brine (TDS ≥ 50 g/L) (Lü et al., 2016; Liu et al., 2017). The main hydrochemical types of fresh water are Cl·HCO_3·SO_4-Ca·Na, Cl-Ca·Na, HCO_3-Ca·Na and HCO_3·SO_4·Cl-Na. The hydrochemical types of brackish water, saline water and brine are Cl-Na·Ca, Cl-Na·Mg, Cl·SO_4-Na and Cl-Na.

2.1.3 Saline water intrusion (SWI)

Our previous studies have verified that SWI is the main groundwater environmental issue in this study area and has negative effects on groundwater quality (Liu et al., 2017; Yang et al., 2021). Because of overexploitation of underground fresh water and the widespread distribution of underground saline water which has been formed from Late Pleistocene, SWI has occurred, and a saline-fresh water mixing zone (SFMZ) has formed, which can lead to groundwater salinity and deterioration of groundwater quality (Liu et al., 2017). Moreover, other human activities can also affect groundwater quality, such as irrigation and sewage discharge. The direct impacts are that groundwater quality is becoming unsuitable for local residents to drink, having a negative impact on human health.

2.2 Sampling and analysis

A total of 47 groundwater samples, which were mainly collected by civilian wells, groundwater monitoring wells and irrigation wells, were collected from May to June 2021 in the SFMZ from the SLB (Fig. 1). Groundwater samples were collected and stored in polyethylene bottles (1200 mL) in a low-temperature environment, and all groundwater samples were sent to the laboratory for testing and analysis for the first

time.

Hydrochemical data were obtained by using test instruments such as UV-visible spectrophotometer (T9CS), Inductive coupled plasma optical emission spectroscopy (iCAP 7400), Atomic fluorescence photometer (XGY-1011A), Ion chromatograph (ICS-600), Inductively coupled plasma mass spectrometer (Thermo iCAP RQ), and Ion meter (PXSJ-216) (Table S1).

2.3 Hydrogeochemical characteristics groundwater quality index (WQI)

The WQI, which is the most widely reliable comprehensive analysis for evaluating drinking water quality, is used to evaluate the groundwater quality (Abbasnia et al., 2019; Nong et al., 2020; Singh et al., 2020; Alshehri et al., 2021). The determined WQI values were then classified into five categories: excellent (WQI < 50); good (WQI = 50–100); poor (WQI = 100.1–200); very poor (WQI = 200.1–300); and unsuitable for drinking water (WQI > 300) (Njuguna et al., 2020; Githaiga et al., 2021).

$$W_i = w_i / \Sigma w_i \quad (1)$$

$$q_i = (C_i / S_i) \times 100 \quad (2)$$

$$SI_i = W_i \times q_i \quad (3)$$

$$WQI = \Sigma SI_i \quad (4)$$

where W_i represents the relative weight, w_i represents the weight that is often allocated to each parameter (Table 1), $\sum w_i$ represents the sum of the weights of all 11 parameters, C_i represents the detected concentration for each parameter in each sample, S_i represents the WHO maximum allowable limits for each parameter, and SI_i represents the water quality subindex of the ith parameter.

2.4 Health risk assessment

Health risk assessment is very important for understanding the potential health risks of chemical pollutants to human beings and is an important basis for local governments to formulate policies or regulations to protect the health of residents (Hu et al., 2021). Health risk assessments include carcinogen risk assessment and noncarcinogen risk assessment. According to International Agency for Research on Cancer (IARC) and Integrated Risk Information System (IRIS) databases, typical pollutants are classified as noncarcinogenic substances and carcinogenic substances (Sadeghfam et al., 2021). Mn, Fe, Pb, Cu, Zn, F^-, NO_3-N, Cl^-, NO_2-N, and Se are classified as noncarcinogenic pollutants, and Cr, As and Cd are classified as carcinogenic pollutants in this study area. Based on the water quality health risk assessment model proposed by the United States Environmental Protection Agency (USEPA), the possible health effects of typical pollutants in inland water on adults and children are evaluated by combining noncancer hazard quotient index (HQ_i) values and carcinogenic risk index (CR_i) values (Hu et al., 2020). This method was used to quantitatively describe whether several groundwater chemical pollutants are present in the SFMZ. The calculation formulas for HQ_i and CR_i of typical pollutants are as follows (Li et al., 2014):

$$CDD_i = \frac{MC_i \times IR \times EF \times ED}{BW \times AT} \tag{5}$$

$$HQ_i = \frac{CDD_i}{R_f D_i} \tag{6}$$

$$CR_i = CDD_i \times SF_i \tag{7}$$

$$HQ = \sum_{i=1}^{n} HQ_i \quad (8)$$

$$CR = \sum_{i=1}^{n} CR_i \quad (9)$$

where CDD_i is the exposure dose through drinking water, mg/(kg·d); MC_i is the average mass concentration of pollutants in water, mg/L; IR is the intake rate, L/d; EF is the exposure frequency, d/a; ED is the duration of exposure, a; BW is human body mass, kg; AT is the average time of exposure, d; R_fD_i is the reference dose of chemical pollutants in the drinking water exposure route, mg/(kg·d); and SF_i is the cancer slope factor, mg/(kg·d).

The parameter value of each variable used in the calculation is based on the data of the risk assessment information system (RAIS) established by the Oak Ridge National Laboratory under the US Department of Energy, as shown in Table S1. The exposure dose was obtained by formula (5), and formulas (6) and (7) were used for pollutant risk assessment. The total health risks of the sampling points were evaluated using equations (8) and (9).

The health risk level of HQ was divided into four levels: (1) HQ ≤ 1, no risk; (2) 1 < HQ ≤ 5, low risk; (3) 5 < HQ ≤ 10, medium risk; and (4) HQ > 10, high risk. According to the USEPA, there is a carcinogenic risk when CR is greater than 1E-4.

2.5 Spatial interpolation

The spatial interpolation analysis algorithm transforms the measured data of discrete points into continuous data surfaces and is widely used in the statistical analysis of geospatial patterns of soil, groundwater and surface water (Horrocks et al., 2021;

Zou et al., 2021). Geostatistics is a branch of applied statistics that focuses on detecting, modeling and estimating spatial patterns in georeferenced data (Qiao et al., 2018). Geostatistics can estimate the values of variables in unsampled regions, and multiple interpolation methods can be used. The inverse distance weighted (IDW) method was adopted in this study. This method combines the advantages of the natural nearest neighbor method based on Tyson polygons and the multiple regression gradient method (Chen and Liu, 2012; Nistor et al., 2020). This method not only considers the distance factor but also assigns weights to discrete observation points near the interpolation point based on the distance. The IDW method is constructed using the following formula (Charizopoulos et al., 2018; Tiwari et al., 2019):

$$\hat{Z}(S_0) = \sum_{i=1}^{n} \lambda_i Z(S_i)$$
$$\lambda_i = \frac{[d(S_i, S_0)] - P}{\sum_{i=1}^{n} [d(S_i, S_0)] - P} \quad (10)$$

where $\hat{Z}(S_0)$ is the predicted value of S_0 (g/kg), $Z(S_i)$ is the measured value of the known point (g/kg), λ_i is the weight, $d(S_i, S_0)$ is the Euclidean distance between the sampling points (m), and P is the specified power.

3. Results

3.1 Groundwater quality types and hydrochemical types

The pH values are 6.94 ~ 8.72 (average 7.68), which indicates a neutral and weakly alkaline environment (Table 2). The TDS values are 266.00 ~ 5082.00 mg/L and 1749.85 mg/L on average. Six groundwater samples are saline water, 10 groundwater samples are fresh water and 31 groundwater samples are brackish water. High-TDS groundwater is distributed in the central and northern parts of the study area (Fig. 2 (a)).

SWI and geochemical processes are responsible for the wide TDS range in this area (Han et al., 2014; Liu et al., 2017).

The hydrochemical types of the saline water are Cl-Na, Cl-Na•Mg, and Cl•SO_4-Na•Ca•Mg. The hydrochemical types of the brackish water are Cl-Na, Cl•HCO_3•SO_4-Ca•Mg, HCO_3•Cl-Ca•Mg, Cl•HCO_3-Na and HCO_3•Cl-Na. The hydrochemical types of the fresh water are HCO_3-Ca•Na, HCO_3•Cl-Na•Mg•Ca, HCO_3•Cl-Na and HCO_3•Cl-Ca•Na•Mg (Fig. 3).

3.2 Spatial distribution of groundwater quality

3.2.1 Nonmental

K^+, Na^+, Ca^{2+}, Mg^{2+}, Cl^-, SO_4^{2-}, HCO_3^-, F^-, NO_3-N and NO_2-N were chosen to analyze the nonmetal groundwater data in this study area.

Na^+, Ca^{2+} and Mg^{2+} concentrations were determined to be in the ranges of 39.37 ~ 1548.41 mg/L, 27.33 ~ 448.45 mg/L and 11.78 ~ 293.30 mg/L, with average values of 350.16 mg/L, 134.88 mg/L and 105.40 mg/L, respectively. Cl^-, SO_4^{2-} and HCO_3^- concentrations were determined to be in the ranges of 32.29 ~ 2171.16 mg/L, 39.13 ~ 992.15 mg/L and 148.01 ~ 927.22 mg/L, with average values of 461.85 mg/L, 261.31 mg/L and 499.07 mg/L, respectively (Table 2). Regions with excess ions were distributed widely in this study area (Fig. 2).

TDS and Cl^- considerations can be used to determine the degree of SWI (Liu et al., 2017). The critical value of TDS was 1000 mg/L, and Cl^- was 250 mg/L. Fig. 2 (a) and (f) show that the TDS and Cl^- considerations are seriously above critical values in most areas, which can indicate that the SWI is prevalent in the groundwater environment of

244 the study area. The main influencing factor is groundwater exploitation (Liu et al.,
245 2017).

246 The F^- concentration was 0.59 ~ 5.41 mg/L, the average value was 2.28 mg/L, and
247 the median value was 2.31 mg/L. Thirty-two groundwater samples had an F
248 concentration above the drinking water guideline value of the WHO (1.5 mg/L), which
249 was 68.1% of the total groundwater samples. This result indicates that the F
250 concentration is very high and can have negative effects on human health. High-F
251 groundwater was mainly found in the central and southern parts of the study area (Fig.
252 2 (i)). The NO_3-N concentration was 0.96 ~ 134.25 mg/L, the average value was 40.39
253 mg/L, and the median value was 35.17 mg/L (Table 2). The areas with excess NO_3-N
254 were mainly distributed in the western and north-central parts of the study area (Fig. 2
255 (j)).

256 3.2.2 Heavy metals

257 Zn, As, Cd, Mn, Fe, Pb and Cu were chosen to analyze the spatial distribution of
258 the metal data of groundwater in this study area. Cd and Mn concentrations were
259 determined to be in the range of 0.05 ~ 24.30 μg/L and 0.0005 ~ 1.62 mg/L, with
260 average values of 1.912 μg/L and 0.086 mg/L, respectively. Some groundwater samples
261 exceeded the WHO standard values. Cd, which exceeded the WHO standard value, was
262 distributed in the central and southeastern parts of the study area. Mn, which exceeded
263 the WHO standard value, was distributed in the northwest corner of the study area (Fig.
264 4). Cd and Mn were the main metal pollutants in this study area and may have negative
265 effects on human health. The Zn, As, Fe, Pb and Cu concentrations were lower than the

WHO standard values and are not a threat to human health.

3.3 Groundwater WQI

Based on existing references and characteristics of the groundwater environment in this study area, we chose K^+, Na^+, Ca^{2+}, Mg^{2+}, Cl^-, SO_4^{2-}, HCO_3^-, F^-, NO_3-N, TDS, Mn and Cd to calculate the groundwater WQI values (Table 3). The calculation results are shown in Table S1 and Fig. 5(a) and (b). The groundwater WQI range was 28.92 ~ 396.22. The groundwater quality was excellent (1 groundwater sample), good (18 groundwater samples), poor (18 groundwater samples), very poor (8 groundwater samples) or unsuitable for drinking water (2 groundwater samples). A total of 40.43% of the total groundwater samples were excellent and good, which was suitable for human drinking. A total of 59.57% of the total groundwater samples were poor, very poor and unsuitable for drinking water (Fig. 5(a)). As shown in Fig. 5(a) and (b), the unsuitable drinking water and very poor water samples were concentrated in the northwestern part of the study area.

4. Discussion

4.1 The direct effects of SWI

Our studies have verified that SWI is the main hydrogeological process in this study area and the main factor that influencing the groundwater quality (Yang et al., 2021). In the SWI process, the main phenomenon is that the TDS and the main ion (Na^+, Ca^{2+} and Cl^-) concentrations increase in the SFMZ (Liu et al., 2017), which can influence the cation exchange in groundwater environment.

Cation exchange, which can drive the enrichment of F^- in groundwater, is an

important process in areas impacted by SWI (Rashid et al., 2018). CAI 1 ($(Cl^-$-$(Na^+$+$K^+))/Cl^-$) and CAI 2 ($(Cl^-$- $(Na^+$+$K^+))/(SO_4^{2-}$+HCO_3^-+NO_3^-+CO_3^{2-})) can illustrate the possibility of cation exchange (Schoeller., 1967; Su et al., 2021). The CAI 1 and CAI 2 values of groundwater samples vary from -1.174 to 0.582 and from -0.001 to 0.0.001, respectively. Only 14 groundwater samples (approximately 33.3% of the total samples) exhibit negative CAI 1 and CAI 2 values, indicating that the cation exchange of Ca^{2+} and Mg^{2+} relative to Na^+ and K^+ in groundwater in the aquifer may not be prevalent and that reverse cation exchange ($2NaX + Ca^{2+} \rightarrow CaX_2 + 2Na^+$) is likely dominant in the study area (Fig. 6 (a)). This process can lead to a decrease in the Ca^{2+} concentration (Chen et al., 2020 b). The role of calcite and dolomite dissolution in groundwater chemistry can be determined by the Ca^{2+}/Mg^{2+} ratio (Li et al., 2018). As shown in Fig. 7, almost all groundwater samples with high F^- concentrations plot below the Ca^{2+}/Mg^{2+} = 1:1 line, which suggests that dolomite dissolution ($CaMg(CO_3)_2 \rightarrow Ca^{2+}+Mg^{2+}+2CO_3^{2-}$) is prevalent in groundwater environment.

4.2 Source of high-F groundwater

According to analysis, high-F groundwater is distributing widely in study area. In coastal areas, groundwater F enrichment is related to the high pH values, high levels of Na^+, HCO_3^-, total dissolved solids (TDS), and salinity and low levels of Ca^{2+} caused by seawater or brine intrusion. High-F groundwater and seawater intrusion have the same distribution pattern, evolution tendency, and associated processes, such as cation exchange (Chen et al., 2014, 2020 b; Wang et al., 2015; Jia et al., 2019).

The Pearson correlation coefficients between F^- and TDS and between F^- and Cl^-

310 are 0.288 and 0.297, respectively. Moreover, the Pearson correlation coefficients
311 between F^- and Na^+, Ca^{2+}, and HCO_3^- are 0.497, -0.340 and 0.349, respectively (Table
312 S2, Fig. S1). These values indicate a higher degree of correlation. It can be speculated
313 that cation exchange may be the main source of groundwater F in the SFMZ
314 (Valenzuela-vásquez et al., 2006; Rashid et al., 2018; Li et al., 2019).

315 Alkaline water can favor the dissolution of F-containing minerals (Lü et al., 2016).
316 The Pearson correlation coefficient between F^- and pH is 0.351, which indicates a
317 positive correlation (Table S2). The groundwater environment in the study area is
318 neutral and weakly alkaline, which is conducive to the enrichment of F^-. The reason is
319 that the surface charge of minerals is neutral or biased negative in alkaline environments,
320 which is not conducive to the adsorption of F^-. The competitive adsorption of OH^- and
321 F^- leads to the release of F^- into groundwater ($Ca(OH)_2 \rightarrow Ca^{2+} + 2OH^-$, $CaF_2 \rightarrow Ca^{2+}$
322 $+ 2F^-$) (Guo et al., 2012). Neutral and weakly alkaline environments are conducive to
323 the enrichment of F^- but are not the main factor.

324 In addition, HCO_3^- is a strong competitively adsorbed ion in alkaline environments
325 (Su and Puls., 2001). The Pearson correlation coefficient between F^- and HCO_3^- is
326 0.349. In this study area, HCO_3^- is at a high concentration (148.01 ~ 927.22 mg/L, with
327 an average of 499.07 mg/L), which is conducive to the release of F^- in CaF_2 attached to
328 mineral surfaces into the groundwater ($CaF_2 + 2HCO_3^- = CaCO_3 + 2F^- + H_2O + CO_2$),
329 resulting in an increase in the groundwater F concentration.

330 In most arid regions of the world, the F^- concentrations in groundwater are
331 generally increased by evaporation (Rashid et al., 2018). Gibbs diagrams showing TDS

values against the content ratios of $Na^+/(Na^+ + Ca^{2+})$ have been widely employed to estimate the three significant natural factors controlling groundwater chemistry: rock weathering, precipitation and evaporation.

Most of the groundwater samples fall into the evaporation dominance area, indicating that evaporation and/or evaporite dissolution have a significant effect on the formation of dissolved solutes (Fig. 6 (b)). The Gibbs diagram shows that most of the samples have $Na^+/(Na^+ + Ca^{2+})$ ratios exceeding 0.5, indicating that cation exchange has significant effects on groundwater chemistry.

To further evaluate the effect of evaporation on the F^- enrichment in the groundwater environment, F^-/Cl^- was plotted against F^- (Fig. 7 (a)). Almost all the groundwater samples have a F^-/Cl^- molar ratio less than the typical value ($F^-/Cl^- = 0.02$) of unpolluted precipitation, which indicates the notable effect of evaporation on F accumulation in the groundwater environment (Currell et al., 2011; Zhang et al., 2020).

The Pearson correlation coefficients between F^- and Na^+ and between F^- and Ca^{2+} are 0.497 and -0.340, respectively. Moreover, the $SI_{fluorite}$ values are 0.08 ~ -1.48 (only one sample is > 0.0) (Fig. 7 (c)), which indicates that the potential for fluorite dissolution is high in the groundwater environment ($CaF_2 \rightarrow Ca^{2+} + 2F^-$). The increase in Na^+ concentration and decrease in Ca^{2+} concentration can promote further dissolution of fluorite and other F-containing minerals, thereby releasing F^- into the groundwater (Su et al., 2013; Liu et al., 2015; Li et al., 2019). In high-F groundwater, dolomite dissolution and increasing F^- concentrations can lead to decreasing $SI_{fluorite}$ values (Fig. 7 (c)), hindering further fluorite dissolution.

Human activity, such as irrigation and agricultural development, is an important factor that influences groundwater quality. Long-term agricultural activities in irrigation districts, including the unreasonable use of pesticides and fertilizers and the deterioration of irrigation water quality, have further worsened the groundwater quality, mainly reflected in the high NO_3-N concentration (Zhang et al., 2021). According to investigations, the main human activity is agricultural irrigation, which can lead to an increase in NO_3-N. The Pearson correlation coefficient between F^- and NO_3-N is -0.185. Hence, there is no obvious relationship between NO_3-N and F^- (Table S2, Fig. S1). It can be speculated that human activity is not the main source of groundwater F.

4.2 Enrichment mechanism of groundwater F in the SFMZ

In the SFMZ, the enrichment mechanism of groundwater F is a relatively complicated process. The characteristics of the groundwater environment, SWI, evaporation and cation exchange are the main factors influencing the enrichment of F. The groundwater environment in the SFMZ is alkaline, which is conducive to the enrichment of F. HCO_3^- is an important component of the groundwater in the study area and is present at relatively high concentrations; these conditions are conducive to the release of F^- from CaF_2 attached to mineral surfaces to the groundwater. Influenced by SWI, the Na^+ and Ca^{2+} concentrations increased in the SFMZ. CaF_2 in the soil or rock is dissolved when the supply of Na^+ and HCO_3^- is adequate through the following reaction: $CaF_2+2HCO_3^-=CaCO_3+2F^-+H_2O+CO_2$, and this process is considered the main mechanism for fluoride leaching. In the SFMZ, reverse cation exchange is prevalent and can reduce the Ca^{2+} concentration. Fluorite dissolution is prevalent in the

groundwater environment, which can lead to an increase in the F concentration. Moreover, evaporation has a notable effect on F^- accumulation in the groundwater environment.

4.3 Health risk assessment and main factors of health risk

Based on groundwater pollutant data, a health risk assessment model and related model parameters were used to calculate the health risk of groundwater in the study area. The carcinogenic risk and noncarcinogenic risk calculation results of each factor are shown in Fig. 8. The average HQ values of typical groundwater pollutants were Cl^->F^->NO_3-N>Se>Mn>NO_2-N>Cu>Pb>Zn>Fe, and the HQ value ranges for adults and children were 11.857~708.545 and 18.213~1088.325 (95.687 and 146.975 on average), respectively. This result indicates that there are high and very high noncarcinogenic risks for adults and children.

The greatest noncarcinogenic risk for adults and children in the study area was caused by Cl^-. The HQ_i values of Cl^- ranged from 10.482 to 704.821 (adults) and 16.101 to 224.314 (children), with averages of 146.040 (adults) and 224.314 (children), accounting for 98.13% of the average HQ values of typical pollutants. Therefore, the HQ_i value of the noncarcinogenic pollutant Cl^- in groundwater greatly exceeded the threshold in the SFMZ, which had negative impacts on the health of adults and children. The second highest contribution to HQ was F^-. The HQ_i values of F^- ranged from 0.479 to 4.390 (adults) and 0.735 to 6.744 (children), and the average values were 1.776 (adults) and 2.728 (children). F^- accounted for 1.19% of the total HQ, which had great impacts on the health of adults and children. Among the indicators of noncarcinogenic

risk, the contribution of NO_3-N to the HQ value was third, with no serious impacts on the health of adults but with a certain impact on the health of children. The HQ_i values of other noncarcinogenic risk indicators, such as Se, Mn, NO_2-N, Cu, Pb, Zn, and Fe, were all lower than the standards and had low impacts on the health of adults and children. Fe had the smallest contribution to the total noncarcinogenic risk, and its contribution to the HQ value was only 0.0022%.

According to the carcinogenic risk index method, Cr, As and Cd were evaluated. The order of the contribution of carcinogenic risk factors according to CR_i was Cd (74.531%)>As (13.123%)>Cr (12.346%). The range of CR values for the total carcinogenic risk of adults and children was 6.148E-05~0.0049 and 9.444E-05~0.0075, and their average CR values were 0.00037 and 0.00057, respectively. In terms of carcinogenic risk level, the total carcinogenic risk in the study area was 4 to 6 orders of magnitude higher than the total noncarcinogenic risk, indicating that the total health risk of groundwater in the study area mainly comes from carcinogenic metal elements. Among these results, the evaluation result of a single index showed that the CRs of Cr and as were less than 1E-4, so their carcinogenic risk could be ignored. Cd was the most important indicator of carcinogenic risk, accounting for 74.531% of the CR. The range of CR values of the Cd index in adults and children was 7.92E-06~0.0048 and 1.217E-05~0.0074, respectively, with an average value of 0.000277~0.000425. The CR_i value of Cd for adults and children exceeded international standards, and the CR value of children was approximately 1.5 times that of adults, indicating that children were at higher risk of carcinogenesis.

Among the noncarcinogenic risks and carcinogenic risks of groundwater, the health risk of children through drinking water is greater than that of adults (Fig. 6). This shows that children are more sensitive risk recipients than adults and are more severely affected by groundwater pollutants. Therefore, children's drinking water safety should be more strictly controlled. According to the USEPA risk standard, the HQ values of adults and children of all groundwater samples exceeded the standard limit. A total of 53.19% of the total groundwater samples in adults exceeded the standard limit, and 97.87% of children exceeded the standard limit. This result indicates that the noncarcinogenic pollutants in the groundwater environment have great negative impacts on the health of adults and children, and the carcinogenic pollutants also have greater impacts on the health of adults and children.

Based on the GIS platform, 6951 randomly distributed sampling points corresponding to 10 index values were extracted from the HQ and CR distribution maps of adults and children. Multiple regression analysis was used to analyze all index values and evaluation results. The calculated correlation coefficient analysis results are listed in Table 4. The results show that Cl^-, which was caused by SWI in this study area, was the most relevant indicator that affects the noncarcinogenic health risks of adults and children. In addition, the regression coefficients of F^-, NO_3-N, Mn, Se and other factors in the area remained above 0.001, which may affect the health risks of residents to a certain extent.

4.4 Spatial distribution of HQ and CR

The HQ values of noncarcinogenic pollutants in adults and children were all higher

than the standards. The polluted areas that seriously affect the health of residents are mainly concentrated on the northwest side of the study area, as shown in Fig. 9. The highest HQ value for adults was 707, and the mean value was 129. A total of 71.25% of the region had HQ values in the 12~129 range. The highest HQ value of children reached 1086, with an average of 198. The HQ values of 68.57% area were in the range of 100~200. The areas where groundwater carcinogenic pollutants had high health effects on adults and children were mainly concentrated in the central region of the study area. The proportion of over-standard areas for adults reached 35.373% of the area, and the proportion of over-standard areas for children reached 44.768% of the area.

In addition, the highest CR value for adults was 0.0049, and the average value was 0.0004. The average value was consistent with international standard health risk limits. The highest CR value for children was 0.0075, and the average value was 0.0007, which was slightly higher than the international standard risk limit. Noncarcinogenic pollutants have definite health effects on the human body, while carcinogenic pollutants may cause CR to exceed the standard in some areas, which has negative effects on human health. The spatial distribution results showed that noncarcinogenic pollutants were enriched in the SFMZ. Compared with carcinogenic pollutants, these noncarcinogenic pollutants had greater impacts on human health.

4.5 The groundwater environmental effects in saline-fresh water mixing zone

Under the conditions of groundwater overexploitation and existence of underground saline water, fresh water and saline water are mixing in groundwater

depression zone and SFMA has formed, which can influence the groundwater environment. In this zone, fresh water, brackish water and saline water are distributing. TDS and Cl^- are the typical environmental pollutants and can reflect the degree of SWI (Liu et al., 2017). Moreover, the concentration values of K^+, Na^+, Ca^{2+}, Mg^{2+}, Cl^-, SO_4^{2-}, HCO_3^- and F are exceeded WHO standard value seriously.

The characteristics of SFMZ is conductive to enrichment of F. An increase in the Na^+ concentration and a decrease in the Ca^{2+} concentration can promote further dissolution of fluorite and other F-containing minerals, releasing F^- into the groundwater. The neutral and weakly alkaline environment is conducive to the enrichment of F^-. High-F groundwater is distributing widely in study area. Agricultural irrigation leads to an increase in nitrate nitrogen in groundwater. Industry has led to an increase in heavy metals in groundwater.

A total of 59.57% of the total groundwater samples were poor, very poor or unsuitable for drinking water. Based on the health risk assessment method, the average HQ sequence in typical groundwater pollutants is $Cl^- > F^- > NO_3$-N > Se > Mn > NO_2-N > Cu > Pb > Zn > Fe, and the CR sequence caused by carcinogenic heavy metals is Cd > As > Cr. In the studied coastal area, the groundwater environment was influenced by the SWI and heavy metal pollution caused by human activity. The Cl^- concentration was extremely high and was the most relevant indicator affecting the noncarcinogenic health risks of adults and children in the area (Fig. 10).

5. Conclusion

In this paper, southern Laizhou Bay is chosen as a case study to explore the

groundwater environmental effects and health risk assessment in saline-fresh water mixing zone of coastal plain. The main conclusions of the study are:

(1) SWI was prevalent in the groundwater environment of the study area, and the main influencing factor was groundwater exploitation. The hydrochemical types of saline water were Cl-Na, Cl-Na • Mg, and Cl • SO_4-Na • Ca • Mg. The hydrochemical types of brackish water were Cl-Na, Cl • HCO_3 • SO_4-Ca • Mg, HCO_3 • Cl-Ca • Mg, Cl • HCO_3-Na and HCO_3 • Cl-Na. The hydrochemical types of fresh water were HCO_3-Ca • Na, HCO_3 • Cl-Na • Mg • Ca, HCO_3 • Cl-Na and HCO_3 • Cl-Ca • Na • Mg. The concentration values of K^+, Na^+, Ca^{2+}, Mg^{2+}, Cl^-, SO_4^{2-}, HCO_3^- and F are exceeded WHO standard value seriously. High-F groundwater was mainly found in the central and southern parts of the study area. Cd and Mn were the main metal pollutants in this study area and may have negative effects on human health. A total of 59.57% of the total groundwater samples were poor, very poor or unsuitable for drinking water.

(2) In the SFMZ in the study area, the groundwater environment, SWI, evaporation and cation exchange are the main factors influencing the enrichment of F. The neutral and weakly alkaline environment is conducive to the enrichment of F^-. Cation exchange and evaporation are the most important factors for the enrichment of F. The supply of Na^+ and HCO_3^- is adequate in the groundwater environment in the study area, which can be conducive to the dissolution of fluorite and subsequent release of F into the groundwater. An increase in the Na^+ concentration and a decrease in the Ca^{2+} concentration can promote further dissolution of fluorite and other F-containing

508 minerals, releasing F^- into the groundwater. Fluorite dissolution is prevalent in this
509 groundwater environment, which can lead to an increase in the F concentration.
510 (3) Based on the health risk assessment method, the average HQ sequence in
511 typical groundwater pollutants is $Cl^- > F^- > NO_3$-N > Se > Mn > NO_2-N > Cu > Pb >
512 Zn > Fe, and the CR sequence caused by carcinogenic heavy metals is Cd > As > Cr.
513 The greatest non-carcinogenic risk to adults and children in the study area is caused by
514 Cl^-. The average HQ of Cl^- is 146.040 (adults) and 224.314 (children), accounting for
515 98.13% of the average total HQ of typical pollutants, which has great impacts on the
516 health of adults and children. Cd is the most important indicator of carcinogenic risk,
517 and its contribution to CR accounts for 74.531%.
518 (4) The HQ values of non-carcinogenic pollutants in groundwater for adults and
519 children are all higher than the standard value, and the pollution areas that seriously
520 affect residents' health are mainly concentrated in the northwest of the study area. The
521 regions with high health impacts of carcinogenic pollutants in groundwater are mainly
522 concentrated in the central part of the study area, with the exceeding range of 35.373%
523 for adults and 44.768% for children. Non-carcinogenic pollutants are enriched in SFMZ,
524 which have greater impacts on human body and lead to higher health risks compared
525 with carcinogenic pollutants.
526 (5) The WQI and health risk assessment methods were combined to assess the
527 water quality and impacts on human health in the SFMZ, and the complementary results
528 exhibited good applicability and accuracy. In the studied coastal area, the groundwater
529 environment was influenced by the SWI and heavy metal pollution caused by human

activity. The Cl^- concentration was extremely high and was the most relevant indicator affecting the noncarcinogenic health risks of adults and children in the area. Effective prevention and control measures to protect groundwater exploitation and prevent SWI, seawater intrusion and discharge of heavy metal pollutants should be of great importance moving forward.

Declarations

Ethics approval and consent to participate

This manuscript does not report on or involve the use of any animal or human data or tissue; therefore, it is not applicable for this part.

Consent for publication

This manuscript does not contain any individual person's data in any form (including any individual details, images or videos); therefore, it is not applicable for this part.

Competing interests

The authors declare no competing interests.

Data availability

Not applicable.

Acknowledgments

This research is financially supported by the National Natural Science Foundation of China (No. 42007166, 41977173), Open Research Fund of State Key Laboratory of Estuarine and Coastal Research (Grant No. SKLEC-KF202010).

Author contribution

Sen Liu: Idea, Conceptualization, Formal analysis, Writing - original draft, Writing -

review & editing. **Xiao Yang**: Formal analysis, Writing - original draft, Writing - review & editing. **Cong Wang**: Investigation, Formal analysis. **Chao Jia**: Writing - review & editing. **Maosheng Gao:** Writing - review & editing. **Xianzhang Dang**: Investigation, Formal analysis, Writing - original draft.

Reference

Abbasnia, A., Yousefi, N., Mahvi, A.H., Nabizadeh, R., Radfard, M., Yousefi, M., Alimohammadi M., 2019. Evaluation of groundwater quality using water quality index and its suitability for assess ing water for drinking and irrigation purposes: case study of Sistan and Baluchistan province (Iran). Human and Ecological Risk Assessment: An International Journal. 25(4), 988-1005. https://doi.org/10.1080/10807039.2018.1458596

Al-Ansari, N., 2013. Management of water resources in Iraq: perspectives and prognoses. Engineering, 5, 667–684

Alshehri, F., Almadani, S., El-Sorogy, A.S., Alwaqdani, E., Alfaifi, H., Alharbi, T., 2021. Influence of seawater intrusion and heavy metals contamination on groundwater quality, Red Sea coast, Saudi Arabia. Marine Pollution Bulletin. 165, 112094. https://doi.org/10.1016/j.marpolbul.2021.112094

Adimalla, N., Qian, H., 2021. Groundwater chemistry, distribution and potential health risk appraisal of nitrate enriched groundwater: a case study from the semi-urban region of South India. Ecotoxicology and Environmental Safety. 207, 111277. https://doi.org/10.1016/j.ecoenv.2020.111277

Chae, G.T., Yun S.T., Mayer B., Kim K.H., Kim S.Y., Kwon J.S., Kim K., Koh Y.K., 2007. Fluorine geochemistry in bedrock groundwater of South Korea. Science of the Total Environment, 385, 272-283. doi:10.1016/j.scitotenv.2007.06.038

Charizopoulos, N., Zagana, E., Psilovikos, A., 2018. Assessment of natural and anthropogenic impacts in groundwater, utilizing multivariate statistical analysis and inverse distance weighted interpolation modeling: the case of a Scopia basin (Central Greece). Environ. Earth Sci. 77. https://doi.org/10.1007/s12665-018-7564-6.

Chen, F., Liu, C., 2012. Estimation of the spatial rainfall distribution using inverse distance

580 weighting (IDW) in the middle of Taiwan. Paddy Water Environ. 10,209-222.
581 https://doi.org/10.1007/s10333-012-0319-1.
582 Chen, Q., Lu, Q.S., Song, Z.J., Chen, P., Cui, Y.K., Zhang, R., Li, X.H., Liu, J.Y., 2014. The levels
583 of fluorine in the sediments of the aquifer and their significance for fluorosis in coastal region
584 of Laizhou Bay, China. Environmental Earth Science. 71(10), 4513–4522.
585 https://doi.org/10.1007/s12665-013- 2843-8
586 Chen, Q., Dong, F.Y., Jia, Z.W., Wei, J.C., Jia, C.P., An, M.G., Ji, Y.H., Hao, D.C., 2020 a. The
587 experimental study of fluorine-leaching ability of granite with different solutions: A new
588 insight into the dynamic of groundwater fluorine levels along coastal zones. Journal of
589 Contaminant Hydrology, 235, 130703. https://doi.org/10.1016/j.jconhyd.2020.103703
590 Chen, Q., Jia, C.P., Wei, J.C., Dong, F.Y., Yang, W.G., Hao, D.C., Jia, Z.W., Ji, Y.H., 2020 b.
591 Geochemical process of groundwater fluoride evolution along global coastal plains: Evidence
592 from the comparison in seawater intrusion area and soil salinization area. Chemical Geology,
593 552, 119779. https://doi.org/10.1016/j.chemgeo.2020.119779
594 Chen, Q., Hao, D.C., Wei, J.C., et al., 2019. Geo-chemical processes during the mixing of seawater
595 and fresh water in estuarine regions and their effect on water fluorine levels. Mausam, 70 (2),
596 329–338.
597 Currell, M., Cartwright, I., Raveggi, M., Han, D.M., 2011. Controls on elevated fluoride and arsenic
598 concentrations in groundwater from the Yuncheng Basin, China. Applied Geochemistry. 26,
599 540-552. https://doi.org/10.1016/j.apgeochem.2011.01.012.
600 Famiglietti, J.S., 2014. The global groundwater crisis. Nature Climatic Change, 4, 945–948.
601 Gao, G.D., Wang, X.H., Bao, X.W., Song, D.H., Lin, X.P., Qiao, L.L., 2017. The impacts of land
602 reclamation on suspended-sediment dynamics in Jiaozhou Bay, Qingdao, China. Estuarine,
603 Coastal and Shelf Science, 206, 61-75. https://doi.org/10.1016/j.ecss.2017.01.012.
604 Githaiga, K.B., Njuguna, S.M., Gituru, R.W., Yan, X., 2021. Water quality assessment, multivariate
605 analysis and human health risks of heavy metals in eight major lakes in Kenya. Journal of

606 Environmental Management. 297, 113410. https://doi.org/10.1016/j.jenvman.2021.113410
607 Guo, H.M., Zhang, Y., Xing, L.N., Jia, Y.F., 2012. Spatial Variation in Arsenic and Fluoride
608 Concentrations of Shallow Groundwater from the Town of Shahai in the Hetao Basin, inner
609 Mongolia. Applied Geochemistry, 27, 2187-2196. DOI:10.1016/j.apgeochem.2012.01.016
610 Han, D.M., Song, X.F., Currell, M.J., Yang, J.L., Xiao, G.Q., 2014. Chemical and isotopic
611 constraints on evolution of groundwater salinization in the coastal plain aquifer of Laizhou Bay,
612 China. J. Hydrol. 508, 12–27. https://doi.org/10.1016/j.jhydrol.2013.10.040.
613 Horrocks, T., Holden, E., Wedge, D., Wijns, C., 2021. 3-D geochemical interpolation guided by
614 geophysical inversion models. Geoscience Frontiers 12,101089.
615 https://doi.org/10.1016/j.gsf.2020.09.018.
616 Hu, G., Rana, A., Mian, H.R., Saleem, S., Mohseni, M., Jasim, S., Hewage, K., Sadiq, R., 2020.
617 Human health risk-based life cycle assessment of drinking water treatment for heavy
618 metal(loids) removal. J. Clean. Prod. 267,121980.
619 https://doi.org/10.1016/j.jclepro.2020.121980.
620 Hu, G., Liu, H., Chen, C., Li, J., Hou, H., Hewage, K., Sadiq, R., 2021. An integrated geospatial
621 correlation analysis and human health risk assessment approach for investigating abandoned
622 industrial sites. J. Environ. Manage. 293,112891.
623 https://doi.org/10.1016/j.jenvman.2021.112891.
624 Jia, C.P., Chen, Q., Wei, J.C., Wang, H.M., Shi, L.Q., Ning, F.Z., Liu, S.L., Yang, M.Y., Xue, X.,
625 Dong F.Y., 2019. The study on the mechanism of fluorine transformation between water and
626 rock (soil) in seawater intrusion areas based on FTIR spectrum. Spectroscopy and Spectral
627 Analysis, 39 (4), 1036–1040. https://doi.org/10.3964/j.issn.1000-0593(2019)04-1036-05.
628 Kim, S.H., Kim, K., Ko, K.S., Kim, Y., Lee, K.S., 2012. Co-contamination of Arsenic and Fluoride
629 in the Groundwater of Unconsolidated Aquifers Under Reducing Environments. Chemosphere,
630 87(8), 851-856. DOI:10.1016/j.chemosphere.2012.01.025
631 Li, X., Huang, X., Zhang, Y.H., 2021. Spatio-temporal analysis of groundwater chemistry, quality
632 and potential human health risks in the Pinggu basin of North China Plain: Evidence from

high-resolution monitoring dataset of 2015–2017. Science of the Total Environment. 800, 149568. https://doi.org/10.1016/j.scitotenv.2021.149568

Li, P., Tian, R., Xue, C., Wu, J., 2017. Progress, opportunities and key fields for groundwater quality research under the impacts of human activities in China with a special focus on western China. Environmental Science and Pollution Research. 24(15), 13224–13234. https://doi.org/10.1007/s11356-017-8753-7.

Li, P., Wu, J., Tian, R., He, S., He, X., Xue, C., Zhang, K., 2018. Geochemistry, hydraulic connectivity and quality appraisal of multilayered groundwater in the Hongdunzi Coal Mine, Northwest China. Mine Water and the Environment. 37(2), 222–237. https://doi.org/10.1007/s10230-017-0507-8

Li, Z., Ma, Z., van der Kuijp, T.J., Yuan, Z., Huang, L., 2014. A review of soil heavy metal pollution from mines in China: Pollution and health risk assessment. Sci. Total Environ. 468-469,843-853. https://doi.org/10.1016/j.scitotenv.2013.08.090.

Li, P., He, X., Li, Y., Xiang, G., 2019. Occurrence and Health Implication of Fluoride in Groundwater of Loess Aquifer in the Chinese Loess Plateau: A Case Study of Tongchuan, Northwest China. Exposure and Health, 11, 95-107. DOI:10.1007/s1240 3-018-0278-x

Liu, S., Gao, M., Tang, Z., Hou, G. and Guo, F., 2016. Responses of submarine groundwater to silty-sand coast reclamation: A case study in south of Laizhou Bay, China. Estuarine, Coastal and Shelf Science, 181, 51–60. https://doi.org/10.1016/j.ecss.2016.08.012

Liu, S., Tang, Z., Gao, M., Hou, G., 2017. Evolutionary process of saline-water intrusion in Holocene and Late Pleistocene groundwater in southern Laizhou Bay. Science of the Total Environment. 607–608, 586–599. https://doi.org/10.1016/j.scitotenv.2017.06.262.

Liu, H.Y, Guo, H.M, Yang, L.J, Wu, L.H., Li, H.L., Li S.Y., Ni P., Liang X., 2015. Occurrence and formation of High Fluoride Groundwater in the Hengshui Area of the North China Plain. Environmental Earth Sciences, 74(3), 2329-2340. DOI:10.1007/s12665-015-4225-x

Lu, J., Wu, J., Zhang, C., Zhang, Y., 2020. Possible effect of submarine groundwater discharge on the pollution of coastal water: occurrence, source, and risks of endocrine disrupting chemicals

660 in coastal groundwater and adjacent seawater influenced by reclaimed water irrigation.
661 Chemosphere, 250, 126323. https://doi.org/10.1016/j.chemosphere.2020.126323
662 Lü, J., Qiu, H.Y., Lin, H.B., Yuan, Y., Chen, Z., Zhao, R.R., 2016. Source apportionment of fluorine
663 pollution in regional shallow groundwater at You'xi County southeast China. Chemosphere,
664 158, 50-55. http://dx.doi.org/10.1016/j.chemosphere.2016.05.057
665 Luo, Y.F, Xiao, Y., Hao, Q.C, Zhang, Y.H, Zhao, Z., Wang, S.B, Dong, G.F, 2021. Groundwater
666 geochemical signatures and implication for sustainable development in a typical endorheic
667 watershed on Tibetan plateau. Environmental Science and Pollution Research. 28, 48312-
668 48329. https://doi.org/10.1007/s11356-021-14018-x
669 Manoj, S., RamyaPriya, R., Elango, L., 2021. Long-term exposure to chromium contaminated
670 waters and the associated human health risk in a highly contaminated industrialised region.
671 Environmental Science Pollution Research. 28, 4276–4288. https://doi.org/10.1007/s11356-
672 020-10762-8
673 Mcmahon, P.B., Brown, C.J., Johnson, T.D., Belitz, K., Lindsey, B.D., 2020. Fluoride Occurrence
674 in United States Groundwater. Science of the Total Environment, 732, 139217.
675 DOI:10.1016/j.scitotenv.2020. 139217
676 Mukherjee, I., Singh, U.K., Singh, R.P., 2021. An Overview on Heavy Metal Contamination of
677 Water System and Sustainable Approach for Remediation, Water Pollution and Management
678 Practices. Springer Singapore Singapore, pp. 255–277.
679 Naujokas, M., Anderson, B., Ahsan, H., Aposhian, H.V., Suk, W., 2013. The broad scope of health
680 effects from chronic arsenic exposure: update on a worldwide public health problem.
681 Environmental Health Perspectives. 121, 295–302. https://doi.org/10.1289/ ehp.1205875
682 Nistor, M.M., Rahardjo, H., Satyanaga, A., Hao, K.Z., Xiaosheng, Q., Sham, A.W.L., 2020.
683 Investigation of groundwater table distribution using borehole piezometer data interpolation:
684 Case study of Singapore. Eng. Geol. 271,105590.
685 https://doi.org/10.1016/j.enggeo.2020.105590.
686 Njuguna, S.M., Onyango, J.A., Githaiga, K.B., Gituru, R.W., Yan, X., 2020. Application of
687 multivariate statistical analysis and water quality index in health risk assessment by domestic

use of river water. Case study of Tana River in Kenya. Process Safety and Environmental. Protection, 133, 149–158. https://doi.org/10.1016/j.psep.2019.11.006.

Nong, X.Z, Shao, D.G, Zhong, H., Liang, J.K, 2020. Evaluation of water quality in the Southto-North Water Diversion Project of China using the water quality index (WQI) method. Water Research. 178, 115781. https://doi.org/10.1016/j.watres.2020.115781

Post, V.E.A., 2005. Fresh and saline groundwater interaction in coastal aquifers: Is our technology ready for the problems ahead? Hydrogeological Journal. 13(1), 120–123. http://dx.doi.org/10.1007/s10040-004-0417-2.

Qiao, P., Lei, M., Yang, S., Yang, J., Guo, G., Zhou, X., 2018. Comparing ordinary kriging and inverse distance weighting for soil as pollution in Beijing. Environ. Sci. Pollut. R. 25,15597-15608. https://doi.org/10.1007/s11356-018-1552-y.

Rashid, A., Guan, D.X., Farooqi, A., Khan, S., Zahir, S., Jehan, S., Khattak, S.A., Khan, M.S., Khan, R., 2018. Fluoride prevalence in groundwater around a fluorite mining area in the flood plain of the River Swat, Pakistan. Science of the Total Environment. 635, 203–215. https://doi.org/10.1016/j.scitotenv.2018.04.064

Rezaei, H., Jafari, A., Kamarehie, B., Fakhri, Y., Ghaderpoury, A., Karami, M.A., Ghaderpoori, M., Shams, M., Bidarpoor, F., Salimi, M., 2019. Health risk assessment related to the fluoride, nitrate, and nitrite in the drinking water in the Sanandaj, Kurdistan county, Iran. Human and Ecological Risk Assessment, 25 (5/6), 1242-1250. https://doi.org/10.1080/10807039.2018.1463510

Sadeghfam, S., Abdi, M., Khatibi, R., Nadiri, A.A., 2021. An investigation into uncertainties within Human Health Risk Assessment to gain an insight into plans to mitigate impacts of arsenic contamination. Journal of Cleaner Production, 211, 127667. https://doi.org/10.1016/j.jclepro.2021.127667

Schoeller, H., 1967. Qualitative Evaluation of Groundwater Resources. In: Methods and Techniques of Groundwater investigations and Development UNESCO, Water Resources Series, 33, 44-52.

715 Su, C.M., Puls, R.W., 2001. Arsenate and Arsenite Removal by Zerovalent Iron: Effects of
716 Phosphate, Silicate, Carbonate, Borate, Sulfate, Chromate, Molybdate, and Nitrate, Relative
717 to Chloride. Environmental Science & Technology, 35(22), 4522-4568.
718 DOI:10.1021/es010768z
719 Singh, G., Patel, N., Jindal, T., Srivastava, P., Bhowmik, A., 2020. Assessment of spatial and
720 temporal variations in water quality by the application of multivariate statistical methods in
721 the Kali River, Uttar Pradesh, India. Environmental Monitoring and Assessment. 192, 1–26.
722 https://doi.org/10.1007/s10661-020-08307-0.
723 Sharma, B., Singh, S., Siddiqi, N.J., 2014. Biomedical implications of heavy metals induced
724 imbalances in redox systems. BioMed Research International. 2014, 1–26.
725 https://doi.org/10.1155/2014/640754
726 Sharma, S., Nagpal, A.K., Kaur, I., 2019. Appraisal of heavy metal contents in groundwater and
727 associated health hazards posed to human population of Ropar wetland, Punjab, India and its
728 environs. Chemosphere 227, 179–190. https://doi.org/10.1016/j.chemosphere.2019.04.009
729 Solgi, E., Jalili M., 2021. Zoning and human health risk assessment of arsenic and nitrate
730 contamination in groundwater of agricultural areas of the twenty two village with geostatistics
731 (Case study: Chahardoli Plain of Qorveh, Kurdistan Province, Iran). Agricultural Water
732 Management, 255, 107023. https://doi.org/10.1016/j.agwat.2021.107023
733 Sanford, W.E., Pope, J.P., 2010. Current challenges using models to forecast seawater intrusion:
734 lessons from the Eastern Shore of Virginia, USA. Hydrogeological Journal. 18(1), 73–93.
735 http://dx.doi.org/10.1007/s10040-009-0513-4
736 Thapa, R., Gupta, S., Gupta, A., 2018. Geochemical and geostatistical appraisal of fluoride
737 contamination: an insight into the quaternary aquifer. Science of the Total Environment. 640,
738 406–418. https://doi.org/10.1016/j.scitotenv.2018.05.360.
739 Tiwari, S., Kumar Jha, S., Sivakumar, B., 2019. Reconstruction of daily rainfall data using the
740 concepts of networks: Accounting for spatial connections in neighborhood selection. J. Hydrol.
741 579,124185. https://doi.org/10.1016/j.jhydrol.2019.124185.
742 Wang Z.Y., Su Q., Wang S., Gao Z.J., Liu J.T., 2021. Spatial distribution and health risk assessment

of dissolved heavy metals in groundwater of eastern China coastal zone. Environmental Pollution, 290, 118016. https://doi.org/10.1016/j.envpol.2021.118016

Wang, Z.Y, Gao, Z.J, Wang, S., Liu, J.T, Li, W., Deng, Q.J, Lv, L., Liu, Y.Q, Su, Q., 2021. Hydrochemistry characters and hydrochemical processes under the impact of anthropogenic activity in the Yiyuan city, Northern China. Environmental Earth Science. 80, 60. https://doi.org/10.1007/s12665-020-09361-0

Wen, X.H, Lu, J., Wu, J., Lin, Y.C, Luo, Y.M, 2019. Influence of coastal groundwater salinization on the distribution and risks of heavy metals. Science of the Total Environment. 652, 267–277. https://doi.org/10.1016/j.scitotenv.2018.10.250

Yadav, K.K., Kumar, S., Pham, Q.B., et al., 2019. Fluoride Contamination, Health Problems and Remediation Methods in Asian Groundwater: a Comprehensive Review. Ecotoxicology and Environmental Safety, 182, 109362. DOI:10.1016/j. ecoenv.2019.06.045

Yang, F., Liu, S., Jia, C., Gao, M.S., Chang, W.B., Wang, Y.J., 2021. Hydrochemical characteristics and functions of groundwater in southern Laizhou Bay based on the multivariate statistical analysis approach. Estuarine, Coastal and Shelf Science, 250, 107153. https://doi.org/10.1016/j.ecss.2020.107153

Valenzuela-vásquez, L., Ramirez-Hernández, J., Reyes-lópez, J., Sol-Uribe, A., LázaroMancilla, O., 2006. The origin of fluoride in groundwater supply to Hermosillo City, Sonora, Mexico. Environmental Geology. 51, 17–27. DOI 10.1007/s00254-006-0300-7

Zhang, Q.Y, Xu, P.P, Qian, H., Yang, F.X, 2020. Hydrogeochemistry and fluoride contamination in Jiaokou Irrigation District, Central China: assessment based on multivariate statistical approach and human health risk. Science of the Total Environment. 741, 140460. https://doi.org/10.1016/j.scitotenv.2020.140460.

Zhang, Q.Y., Xu, P.P., Chen, J., Qian, H., Qu, W.G., Liu, R., 2021. Evaluation of groundwater quality using an integrated approach of set pair analysis and variable fuzzy improved model with

768 binary semantic analysis: A case study in Jiaokou Irrigation District, east of Guanzhong Basin,
769 China. Science of the Total Environment. 767, 145247.
770 https://doi.org/10.1016/j.scitotenv.2021.145247
771 Zou, W., Yin, S., Wang, W., 2021. Spatial interpolation of the extreme hourly precipitation at
772 different return levels in the Haihe River basin. J. Hydrol. 598, 126273.
773 https://doi.org/10.1016/j.jhydrol.2021.126273.

774 Figure captions

775 Figure 1. Location of study area and groundwater samples. (DEM and DEM data is derived from
776 global bathymetric data).

777 Figure 2. The spatial distribution of Non-metal data. (a), TDS; (b), K^+; (c), Na^+; (d), Ca^{2+}; (e), Mg^{2+};
778 (f), Cl^-; (g), SO_4^{2-}; (h), HCO_3^-; (i), F^-; (j), NO_3-N; (k), Se; (l) NO_2-N.

779 Figure 3. The Piper program of groundwater samples in study area

780 Figure 4. The spatial distribution of heavy metals. (a), Zn; (b), As; (c), Cd; (d), Mn; (e), Fe; (f), Pb.
781 (g), Cu.

782 Figure 5. WQI result distribution: (a) WQI value of each sampling point; (b) WQI spatial
783 distribution; (c) WQI value and main factor (Cl^-, F^-, NO_3-N and Cd) distribution chart.

784 Figure 6. (a), Scatterplots of CAI 1 versus CAI 2 to verify cation exchange; (b) Gibbs diagram of
785 groundwater samples.

786 Figure 7. (a) Plots of F^-/Cl^- versus F^- to clarify the role of evaporation in the formation of high-F
787 groundwater; (b) Ca^{2+} versus Mg^{2+} to evaluate the role of calcite and dolomite dissolution in
788 groundwater chemistry; (c) The relationship between $SI_{fluorite}$ and F^-.

789 Figure 8 Evaluation results of each risk factor: (a) noncancer hazard quotient indices; (b)
790 carcinogenic risk indices; (c) Health risk assessment at each point.

791 Figure 9 The distribution of Adult_HQ, Adult_CR, Child_HQ and Child_ CR.

792 Figure 10. The conceptual model of groundwater environmental effects in saline-fresh water mixing
793 zone.

Table Captions

Table 1. The weight, relative weight and WHO standards of each of the parameters used for the WQI determination.

Table 2. Minimum, median, maximum and average values of heavy metals and chemical variables in 47 groundwater samples.

Table 3. The weights each of the parameters used for the WQI determination.

Table 4. The regression coefficient of each factor.

Figures

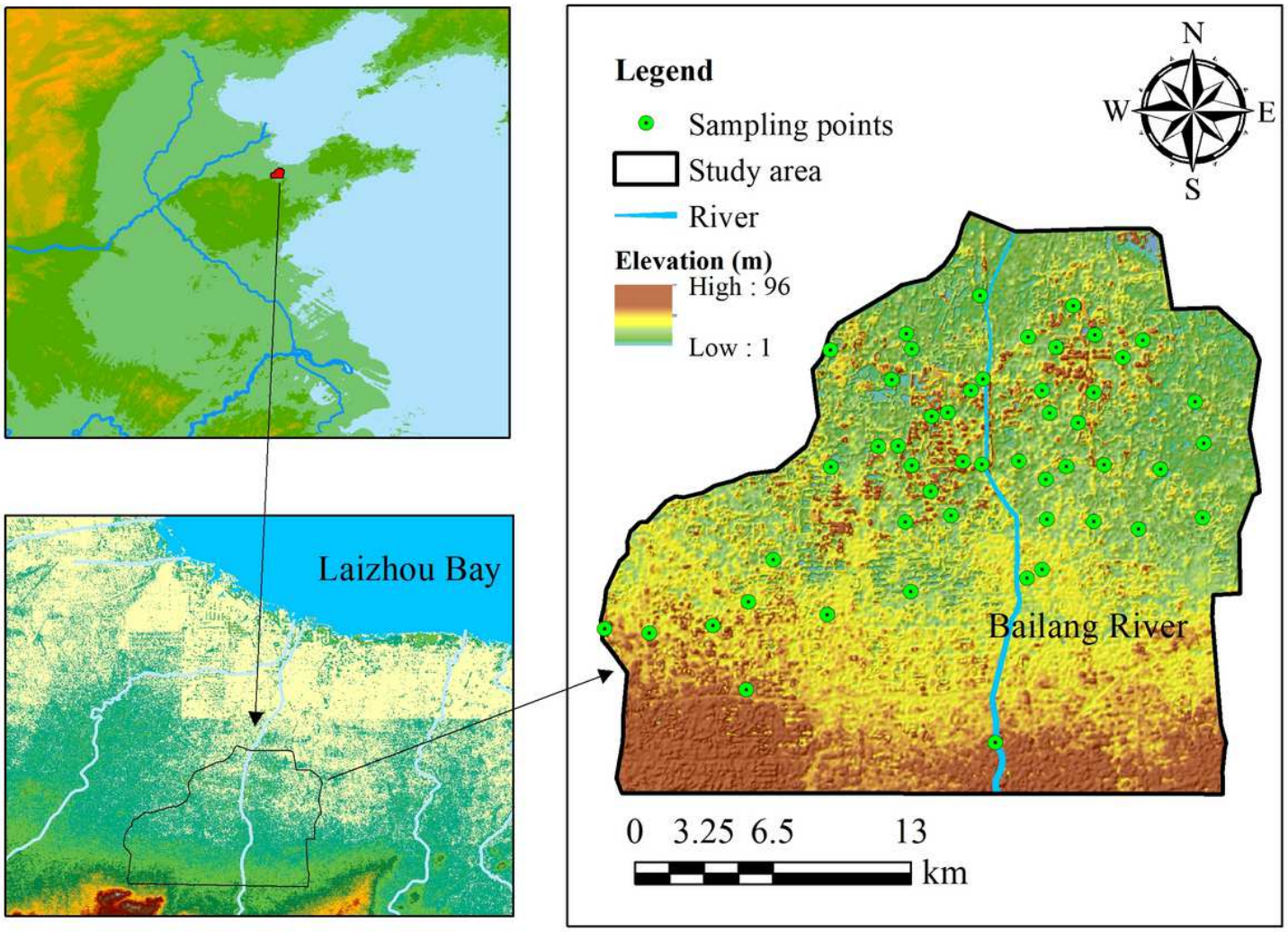

Figure 1

Location of study area and groundwater samples. (DEM and DEM data is derived from global bathymetric data).

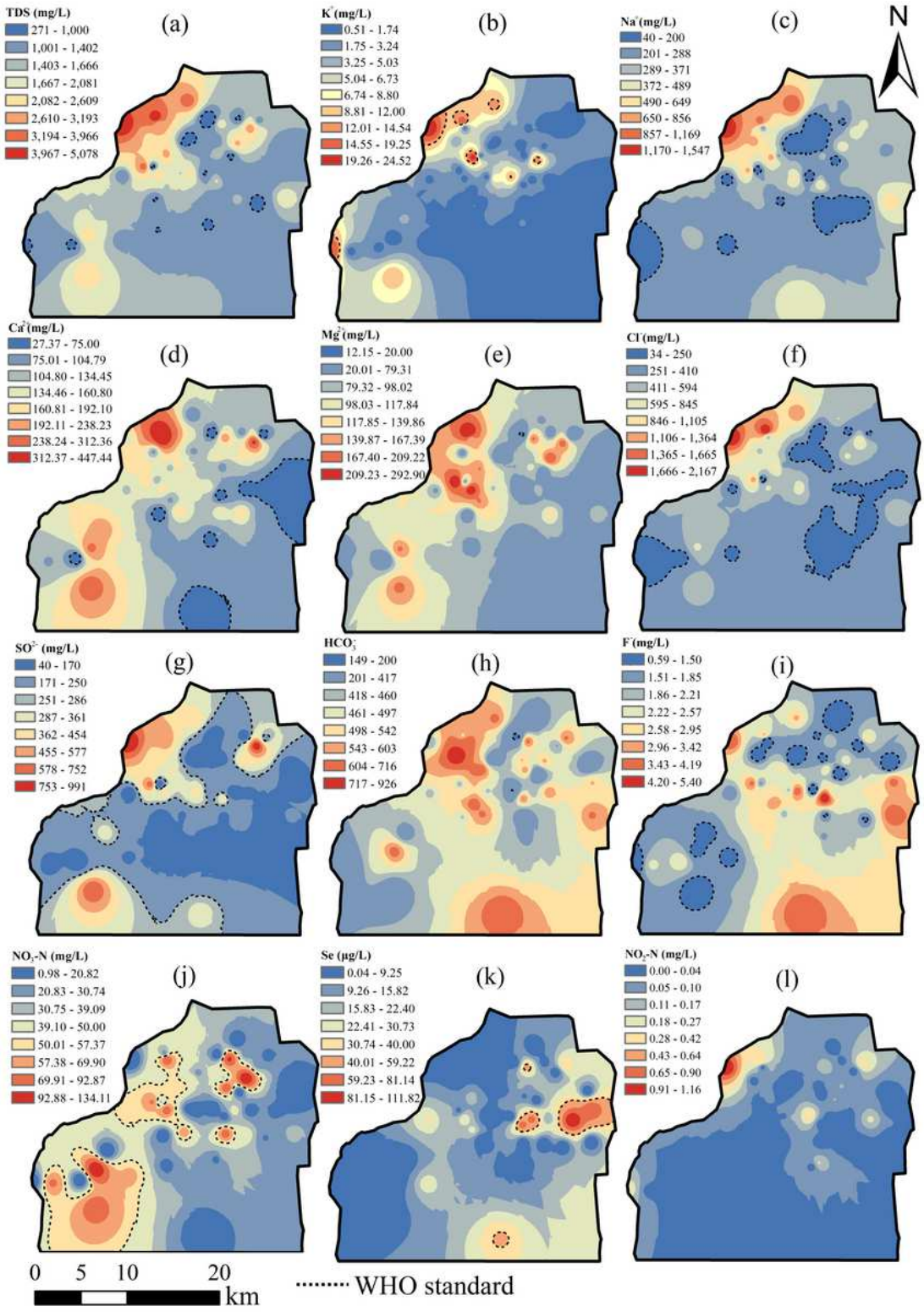

Figure 2

The spatial distribution of Non-metal data. (a), TDS; (b), K^+; (c), Na^+; (d), Ca^{2+}; (e), Mg^{2+}; (f), Cl^-; (g), SO_4^{2-}; (h), HCO_3^-; (i), F^-; (j), NO_3-N; (k), Se; (l) NO_2-N.

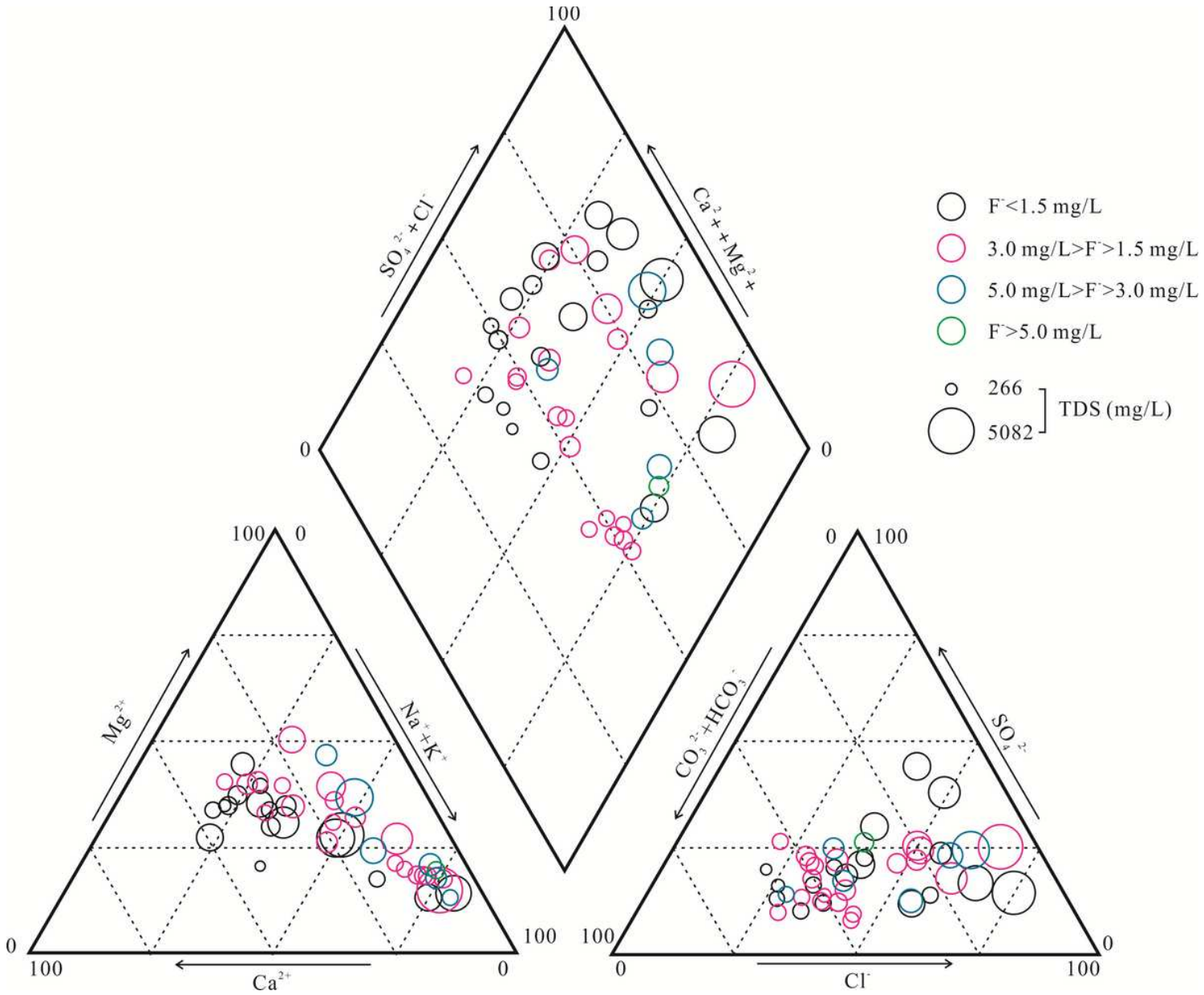

Figure 3

The Piper program of groundwater samples in study area

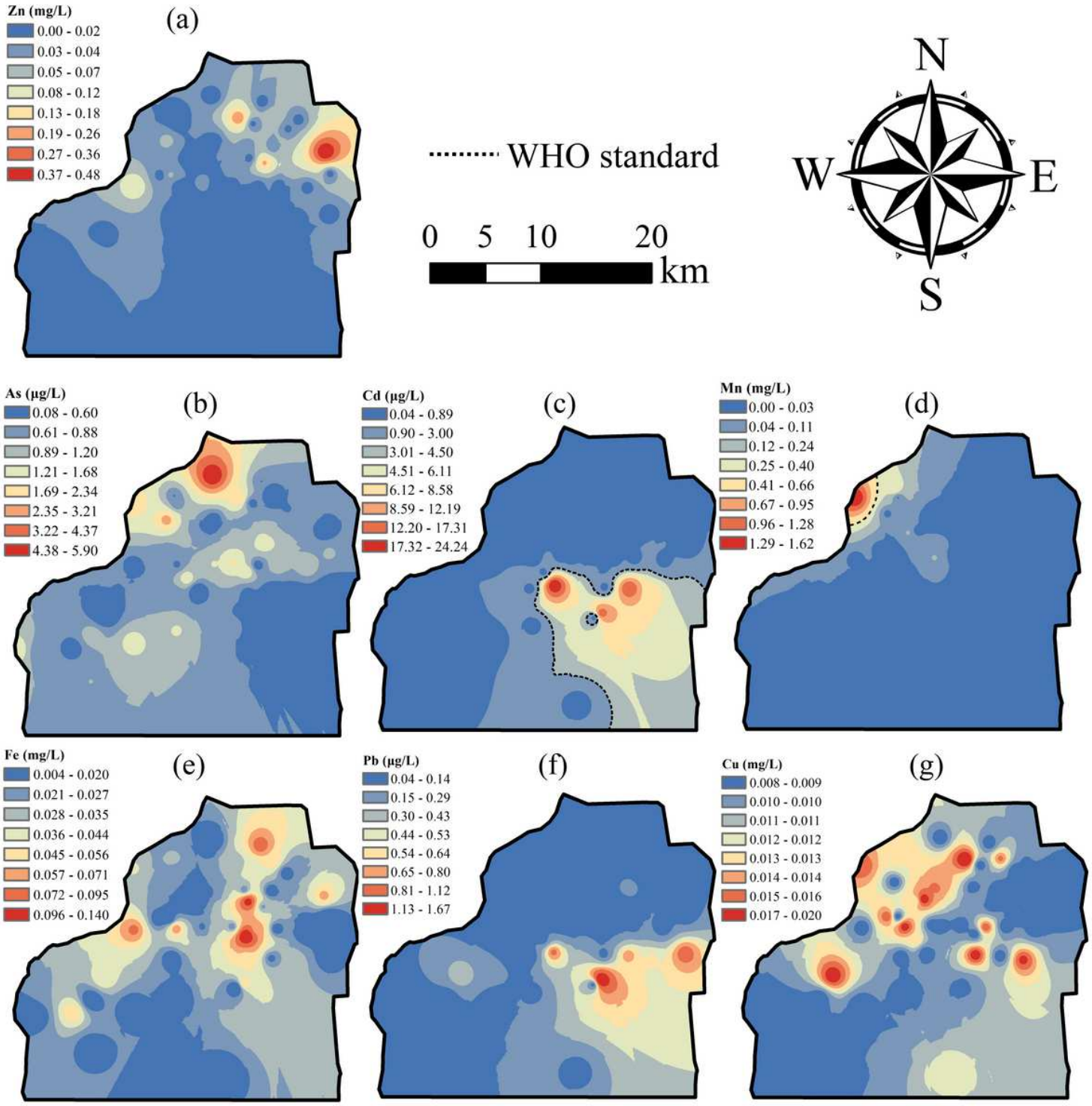

Figure 4

The spatial distribution of heavy metals. (a), Zn; (b), As; (c), Cd; (d), Mn; (e), Fe; (f), Pb. (g), Cu.

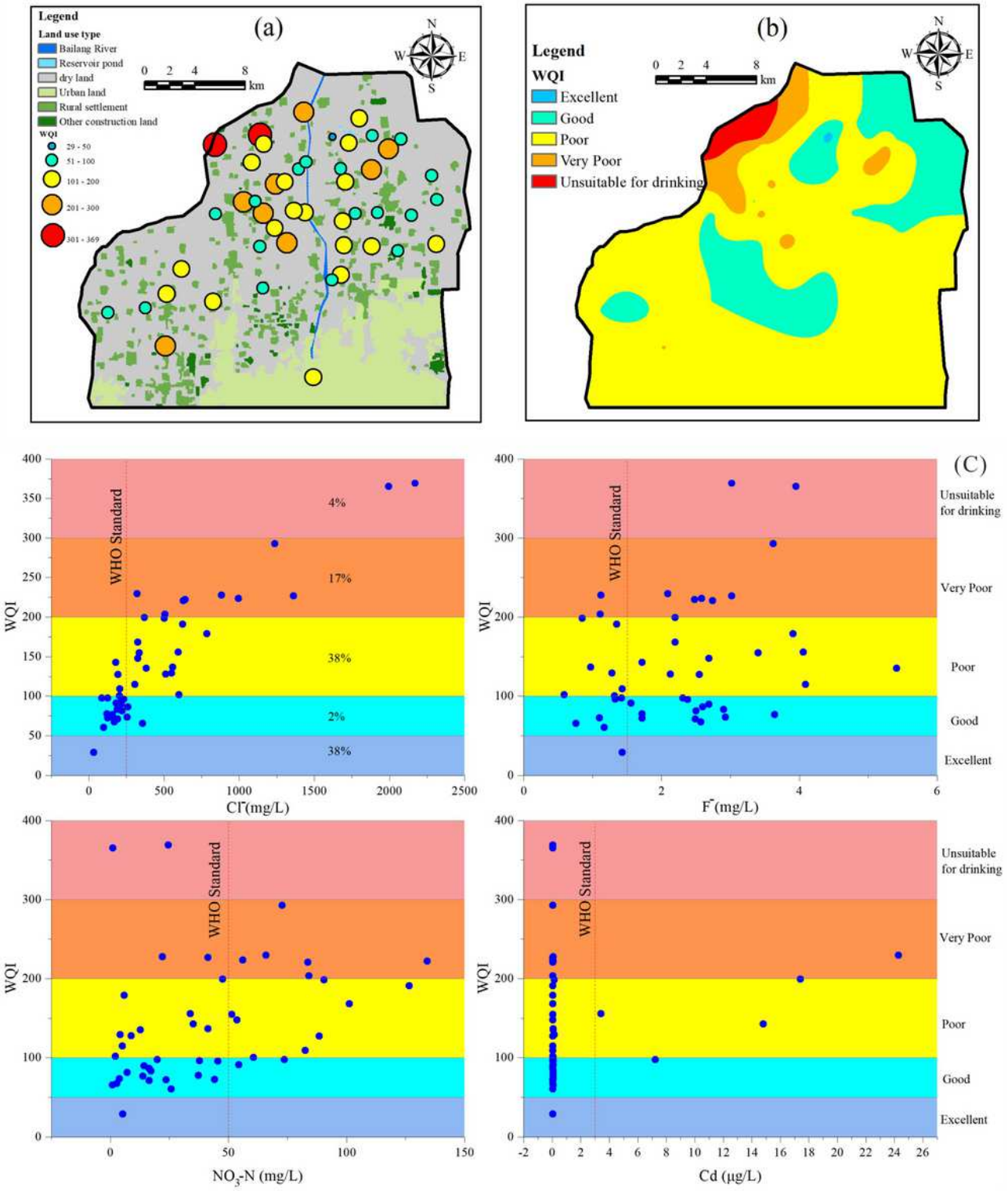

Figure 5

WQI result distribution: (a) WQI value of each sampling point; (b) WQI spatial distribution; (c) WQI value and main factor (Cl^-, F^-, NO_3-N and Cd) distribution chart.

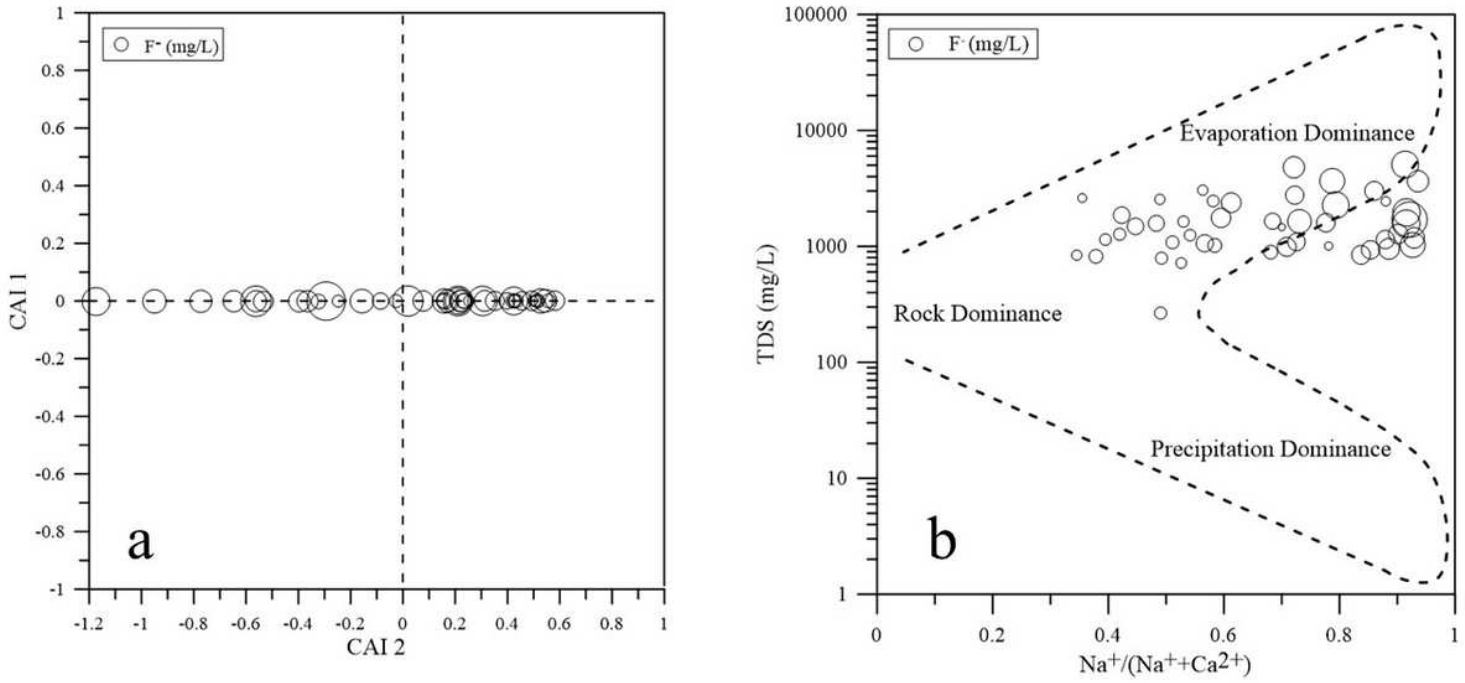

Figure 6

(a), Scatterplots of CAI 1 versus CAI 2 to verify cation exchange; (b) Gibbs diagram of groundwater samples.

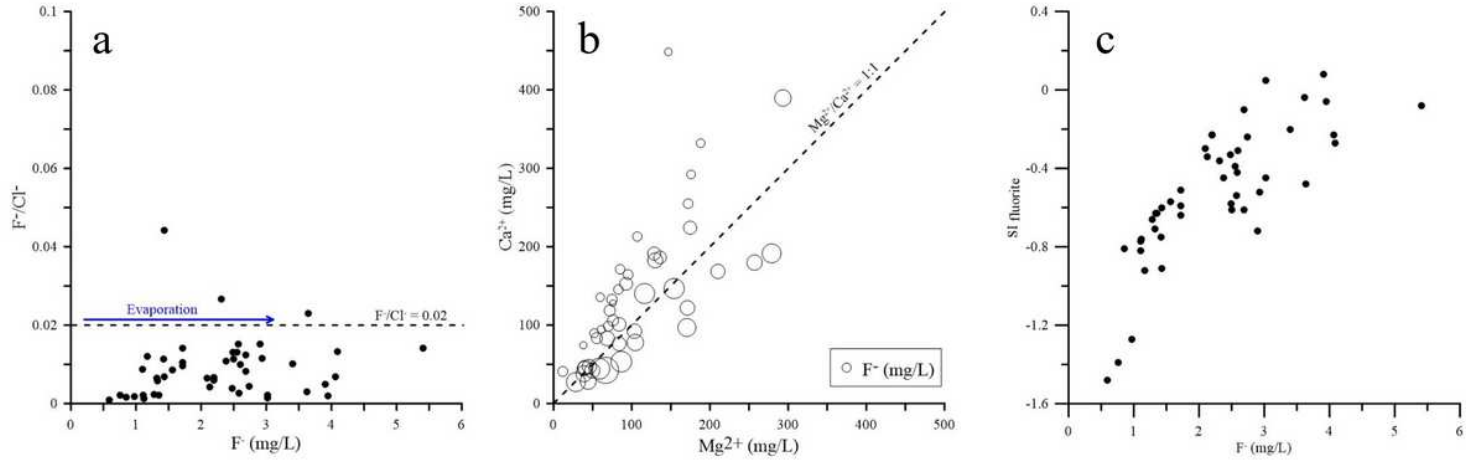

Figure 7

(a) Plots of F^-/Cl^- versus F^- to clarify the role of evaporation in the formation of high-F groundwater; (b) Ca^{2+} versus Mg^{2+} to evaluate the role of calcite and dolomite dissolution in groundwater chemistry; (c) The relationship between $SI_{fluorite}$ and F^-.

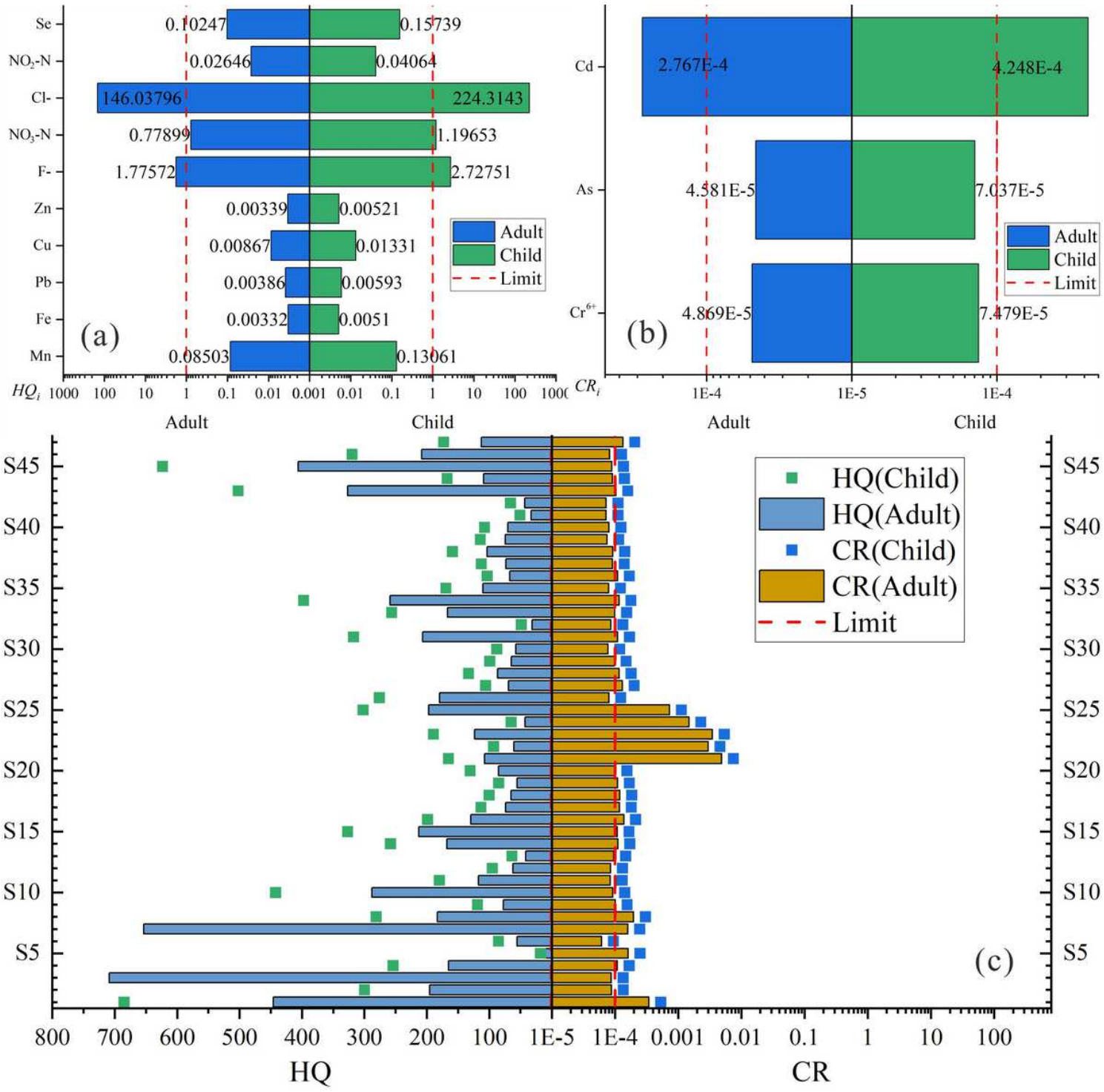

Figure 8

Evaluation results of each risk factor: (a) noncancer hazard quotient indices; (b) carcinogenic risk indices; (c) Health risk assessment at each point.

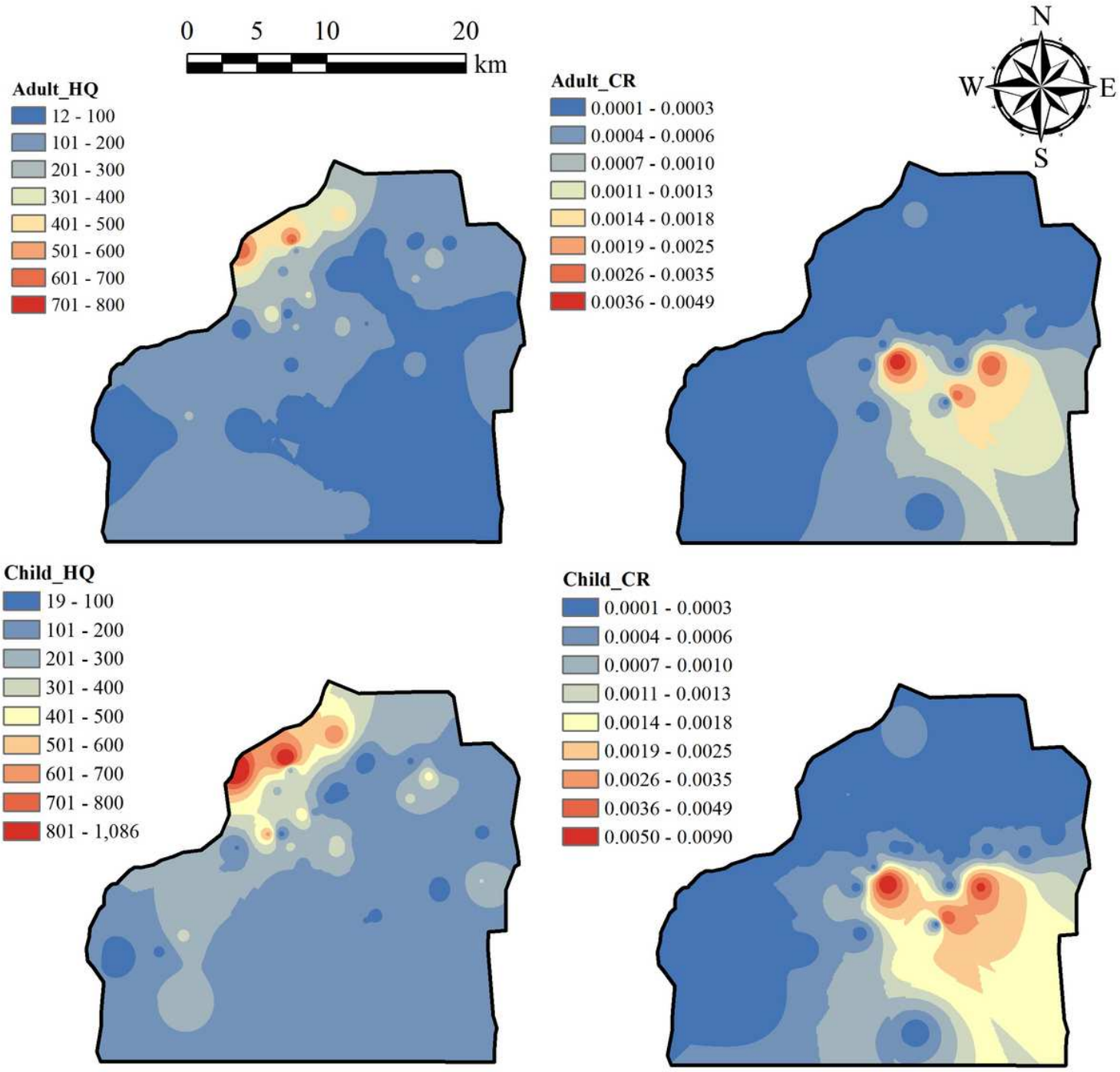

Figure 9

The distribution of Adult_HQ, Adult_CR, Child_HQ and Child_ CR.

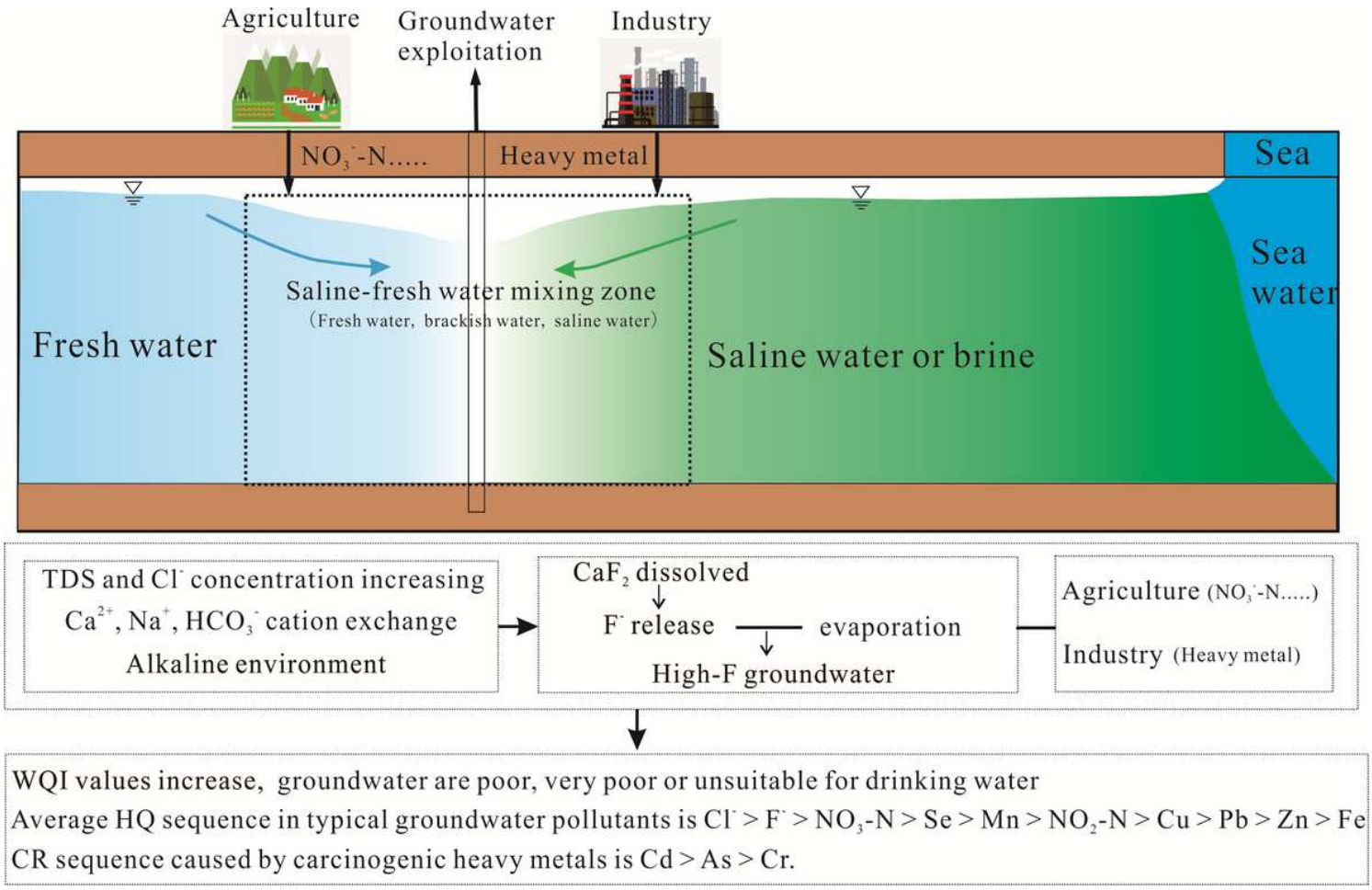

Figure 10

The conceptual model of groundwater environmental effects in saline-fresh water mixing zone.

Supplementary Files

This is a list of supplementary files associated with this preprint. Click to download.

- Supplementarymaterial.docx